Role of the phospholipid binding sites, PX of p47 phox and PB region of Rac1, in the formation of the phagocyte NADPH oxidase complex NOX2

Dina Al Abyad, Xavier Serfaty, Pauline Lefrançois, Stéphane Arbault, Laura Baciou, Sophie Dupre-Crochet, Achraf Kouzayha, Tania Bizouarn

BBA Biomembranes

Role of the phospholipid binding sites, PX of p47^{phox} and PB region of Rac1, in the formation of the phagocyte NADPH oxidase complex NOX2

Dina Al Abyad[1,2], Xavier Serfaty[1], Pauline Lefrançois[3], Stephane Arbault[3,4], Laura Baciou[1], Sophie Dupré[1], Achraf Kouzayha[2] and Tania Bizouarn[1]

[1] *Université Paris Saclay, Institut de Chimie Physique UMR 8000, CNRS, 91405 Orsay Cedex, France.*[1]
[2] *Laboratory of Applied Biotechnology (LBA3B), AZM Center for Research in Biotechnology and its Applications, Doctoral School for Sciences and Technology, Lebanese University, Tripoli 1300, Lebanon.*
[3] *Univ. Bordeaux, Bordeaux INP, CNRS, ISM, UMR 5255, F-33402 Talence, France*
[4] *Univ. Bordeaux, CNRS, Bordeaux INP, CBMN, UMR 5248, F-33600 Pessac, France*

ARTICLE INFOS

Keywords:
NADPH oxidase,
phagocyte,
PLB-985,
lipid-protein interaction,
GUV,
protein complex assembly

ABSTRACT

In phagocytes, superoxide anion ($O_2^{\bullet-}$), the precursor of reactive oxygen species, is produced by the NADPH oxidase complex to kill pathogens. Phagocyte NADPH oxidase consists of the transmembrane cytochrome b_{558} (cyt b_{558}) and four cytosolic components: p40^{phox}, p47^{phox}, p67^{phox}, and Rac1/2. The phagocyte activation by stimuli leads to activation of signal transduction pathways. This is followed by the translocation of cytosolic components to the membrane and their association with cyt b_{558} to form the active enzyme.
To investigate the roles of membrane-interacting domains of the cytosolic proteins in the NADPH oxidase complex assembly and activity, we used giant unilamellar phospholipid vesicles (GUV). We also used the neutrophil-like cell line PLB-985 to investigate these roles under physiological conditions. We confirmed that the isolated proteins must be activated to bind to the membrane. We showed that their membrane binding was strengthened by the presence of the other cytosolic partners, with a key role for p47^{phox}. We also used a fused chimera consisting of p47^{phox}(aa 1-286), p67^{phox}(aa 1-212) and Rac1Q61L, as well as mutated versions in the p47^{phox} PX domain and the Rac polybasic region (PB). We showed that these two domains have a crucial role in the trimera membrane-binding and in the trimera assembly to cyt b_{558}. They also have an impact on O_2.- production *in vitro* and *in cellulo*: the PX domain strongly binding to GUV made of a mix of polar lipids; and the PB region strongly binding to the plasma membrane of neutrophils and resting PLB-985 cells.

1. Introduction

Phagocyte cells destroy pathogens using various molecules and mechanisms. The main microbicidal mechanism starts with the enzymatic production of superoxide anion, the precursor of other reactive oxygen species such as H_2O_2 and HOCl. The NADPH oxidase enzyme, which catalyzes the superoxide anion production, is a multimeric enzyme. It is composed of two transmembrane proteins, Nox2 and p22^{phox} forming the flavocytochrome b_{558} (cyt b_{558}), and four cytosolic proteins, p40^{phox}, p47^{phox}, p67^{phox}, and Rac1 or Rac2. Superoxide anions are generated in phagocytes only in response to soluble stimuli or upon phagocytosis that activate signaling pathways. Despite the availability of all the necessary components: NADPH, O_2 and the proteins forming the NADPH oxidase complex, no superoxide is produced in the resting cells as a consequence of a tightly controlled and complex activation mechanism [1-3]. The control of superoxide anion formation is mainly achieved by keeping separate the various proteins of the NADPH oxidase complex in different subcellular localization. Thus, the NADPH oxidase complex only assembles in response to specific signals. The formation of an active NADPH oxidase enzyme can be divided into three steps. First, a series of post-translational modifications of the soluble proteins occurs, such as phosphorylation of serine residues, 10 have been identified on p47^{phox} [4, 5], threonine such as thr233 for p67^{phox} [4, 6, 7], GDP-GTP exchange on Rac [8, 9] inducing conformational changes that make accessible protein binding sites [10, 11] and lipid binding sites [12, 13]. These changes include the detachment of a GDI protein from Rac that allows the prenyl group present on Cys189 to bind to the membrane. Second, the phospholipid membrane

[1] Corresponding author: Tania Bizouarn, Institut de Chimie Physique, bat 350 Université Paris Saclay, 91405 Orsay, France; email: tania.bizouarn@universite-paris-saclay.fr

Abbreviations : aa, amino acid; AA, arachidonic acid; GUV, giant unilamellar vesicles; cyt b_{558}, flavocytochrome b_{558}; FP, fluorescent protein; PB, polybasic region; PBS, phosphate buffer saline; PMA, phorbol myristate acetate; PPL, phospholipid; HBSS, Hanks' balanced salt solution; RLU, relative light units, LUT, look-up table; ROS, reactive oxygen species; PX, phox homology domain.

composition is modified mostly by phosphorylation of phosphatidylinositol-4phosphate and phosphatidylinositol-(4,5)bisphosphate [14, 15] and an increase in phosphatidic acid proportion [16-18]. Simultaneously, all the cytosolic proteins migrate to the membrane [19-21] and assemble through a first series of protein-protein and protein-lipid interactions. Third, the assembly of the complex creates a second series of conformation changes of proteins induced by new protein-protein interactions, leading to a fully active complex. *In vitro*, these conformational changes in $p47^{phox}$, $p67^{phox}$ and probably in cyt b_{558} are induced by the addition of amphiphilic molecules such as SDS, LiDS [22], or some fatty acids [23] such as the all-*cis*-arachidonic acid used here. Arachidonic acid has been shown to cause conformational changes similar to those of serine phosphorylation, as seen by circular dichroism [24] or pull-down experiments [25].

During the formation of the NADPH oxidase complex, the binding of each of the three cytosolic proteins $p47^{phox}$, $p67^{phox}$ and Rac, to Nox2-$p22^{phox}$ is stabilized by the presence of the other cytosolic proteins; their dissociation constant for cyt b_{558} is strongly decreased [26, 27]. Moreover, it has also been shown that both the protein-protein *and* protein-lipid interactions contribute to the stabilization of this membrane protein complex. Three of the cytosolic proteins contain lipid binding domains, a PX domain in $p40^{phox}$ [28] and $p47^{phox}$ [12 , 13, 29], and a polybasic (PB) region in Rac [8, 30]. These three lipid-binding domains are important for the translocation of the cytosolic proteins to the cyt b_{558} at a specific localization, depending on the lipid compositions, either to the plasma membrane or to the phagosome [30]. These domains are also important for the assembly of the complex [31]. The PX domain of $p47^{phox}$ has two binding pockets, one specific for phosphatidyl inositol 3,4 bisphosphate (PI3,4P2), the other for phosphatidyl serine (PS) and phosphatidic acid (PA) [29]. The PX domain of $p40^{phox}$ specifically binds to phosphatidylinositol-3phosphate (PI3P) present in endosome and phagosome membranes [32, 33]. The Rac1 and Rac2 polybasic region (PB) consists of 6 or 3 positively charged residues, respectively. The interaction of this region with the membranes cytosolic leaflet is solely electrostatic with the negatively charged head groups of the phospholipids. It has been shown that Rac binding on membranes depends on the number of positive charges in the PB domain: the most positively charged PB binds to the most negatively charged membrane [34, 35]. In neutrophils, the PB region of Rac1-GTP directly targets the plasma membrane due to its high positive charge content while the PB region of Rac2-GTP targets endomembranes such as endosomes and phagosomes [36, 37]. The present work has two objectives: *i)* Study the recruitment behavior of $p67^{phox}$, $p47^{phox}$ and Rac to a membrane *ii)* Further investigate the role of two phospholipid-binding domains, the PX domain of $p47^{phox}$ and the PB domain of Rac1, on recruitment to membranes and on the stabilization and activation of the phagocyte NADPH oxidase complex. To fulfill these aims, experiments have been realized *in vitro* and in living PLB-985 cells. *In vitro*, an original biomimetic membrane system, composed of giant unilamellar vesicles (GUV), was generated to directly visualize the protein localization and protein-lipid interactions under confocal fluorescence microscopy. In addition to experiments on separated $p67^{phox}$, $p47^{phox}$ and Rac1Q61L proteins, the trimeras constructed by Berdichevsky et al. [31] were used to focus on phospholipid interactions, independently of the activation step of the cytosolic proteins and to keep their relative stoichiometry 1:1:1 on cyt b_{558}. The prototype trimera is composed of the truncated $p47^{phox}$ (the PX domain and the two SH3 domains), the truncated $p67^{phox}$ (four TPR domains with the activation domain) and mutated Rac1Q61L, to gain an active state of the three proteins. Three mutated trimeras have been used in this work. The $p47^{phox}$ ΔPX trimera consists of the deletion of the PX domain, therefore $p47^{phox}$ is reduced to only the two SH3 domains; the other two mutated trimeras have changes located in the polybasic region of Rac. In the Rac-mutated trimera called Tri-Rac1-PB2, the Rac1 PB region composed of six contiguous positive charges (KKRKRK) is replaced by the Rac2 PB region composed of three positive charges (RQQKRA). In the Rac-mutated trimera called Tri-Rac1-PB6Q, the six positive charges were replaced by six Gln. This construct has the advantage of allowing the removal of one domain of a protein and keeping all the others, making it possible to study the loss of only one part of each protein. With the isolated proteins, the loss of the $p47^{phox}$ PX domain inhibits the assembly of the remaining part of $p47^{phox}$ to cyt b_{558}.

2. Materials and Methods

2.1 Materials

Cis-Arachidonic acid, Dulbecco Phosphate buffer saline (DPBS, ref D8537); phorbol 12-myristate 13-acetate (PMA), poly-L-lysine hydrobromide was purchased from Sigma-Aldrich (ref P1399, St Quentin, France); NADPH (ref 328742500) from Acros Organics (France); AlexaFluor647-maleimide, phosphate buffer saline (PBS, BP2944-100) from Fisher Scientific (France), Soybean Polar Lipid Extract (ref 541602C) from Avanti Polar Lipids.

2.2 In vitro studies

2.2.1 Plasmids construction

The construction of the plasmid pProEx-Cherry-Rac1Q61L coding for the Cherry-Rac1Q61L fusion protein was obtained by ligation of two inserts into the pProEx vector after digestion with EcoR1 and Kpn1 leading to the SGLRSRD linker between the two proteins. The first insert was obtained by PCR amplification of the gene coding for the red Fluorescent Protein variant Cherry from the red mCherry-C1 vector (Clontech) using the primers forward TAGAATTCATGGTGAGCAAGGGCGAGGAG and reverse TACTCGAGATCTGAGTCCGGAC. The second insert was obtained by PCR amplification of the plasmid coding for the GST-Rac1Q61L using the primers forward ATCTCGAGATCAGGCCATCAAGTGTGTGGTGG and reverse TGAGGTACCTTACAACAGCAGGCATTTTCTC.
The pProEx-turq-p67 plasmid coding for the Turquoise-p67^{phox} fusion protein was a generous gift from Pr. M. Erard (ICP, France) [38]. The plasmids of the prototype and mutants GFP-trimera were generously donated by Pr. E. Pick (Tel Aviv University, Israel) [39]. The trimeras used in this paper consist of the fused proteins GFP, p47^{phox} (aa 1-286), p67^{phox} (1-212) and Rac1 (1-192) in which the punctual mutation Q61L confers a constitutively active form, and the three mutants GFP-trimera p47^{phox} ΔPX domain (aa -286), Rac1 ->Rac2 and Rac1 183Q-188Q described in [39]. For simplification and clarity, the mutants have been called Tri-p47ΔPX, Tri-Rac1-PB2 and Tri-Rac1-PB6Q, respectively. All the constructs have been sequenced (Beckman Genomics, UK) to confirm their identity.

2.2.2 *Expression, purification and labelling of cytosolic proteins.*

The Turquoise-p67^{phox} protein, the cherry-Rac1Q61L and p47^{phox} proteins were expressed in *E. coli* BL21 using the protocol described in [40], except that the bacteria were incubated for 4 hours at 30 °C before IPTG induction and at 20 °C overnight after 0.5 mM IPTG addition. It is important to note that the recombinant Rac proteins (isolated and present in trimera) produced in *E. coli* do not contain a prenyl group. The proteins were purified using ion exchange and Ni-sepharose chromatography as described in [27]. The proteins were protected from light by aluminum foil during the purification. The purity of protein solutions was evaluated by migration in 10 % BisTris-NuPAGE SDS gels (Invitrogen), stained with Coomassie Brilliant Blue. The expression and purification of the trimeras were performed as previously described in [39]. p47^{phox} was labeled with Alexa Fluor™ 647 Maleimide (Invitrogen) by incubation with a ratio of 1:1 mol:mol of the protein with the Alexa in the ice and in the dark for 8 h. The solution was then dialyzed against 5 L of phosphate buffer saline solution (PBS) in the cold room and in the dark for 12 h and stored at -80 °C until use.

2.2.3 *Activity measurements in cell free system*

The superoxide production rate was measured by spectrophotometry, following the NADPH consumption at 340 nm using an extinction coefficient of 6.22 $mM^{-1}\cdot cm^{-1}$. Human neutrophil membrane fractions prepared as described in [41] (4 nM cyt b_{558}, evaluated by differential UV-Vis absorption spectrophotometry [42]) and 300 nM of trimera were incubated in PBS buffer supplemented with 10 mM $MgSO_4$, with varying concentrations of arachidonic acid (AA) at 25 °C for 1 min. The reaction was initiated by the addition of 200 µM NADPH. All data is the average of at least 3 independent measurements. The activities have been plotted in "equivalent mol of $O_2^{\bullet-}$. s^{-1}. mol of cyt b_{558}^{-1} ". This means that the measured rate of NADPH oxidation has been multiplied by a factor 2. A control in presence of 25 unit/mL of catalase has been performed in order to check the absence of effect of H_2O_2 produced by the enzyme on activity measurement.

2.2.4 *GUV formation*

Giant unilamellar vesicles (GUV) were prepared using a modified method from [43]. The method consists briefly of dissolving natural polar lipids (Soybean polar lipid extract, Avanti Polar) in chloroform (typically 3 mg in 300 µL $CHCl_3$) and drying them (4-5 hours under vacuum) in a glass flask (30 mL balloon) to form a thin film of lipid. The film is then rehydrated with Tris-phosphate buffer (Tris-base 5 mM, K_3PO_4 30 mM, KH_2PO_4 30 mM, $MgSO_4$ 1 mM, EDTA 0.5 mM, pH 7.4; 10-fold volume relative to the lipid solution) overnight, then added with glycerol (a 100-fold lower volume than the Tris-buffer) and subsequently sonicated in a bath (Branson 2800) to generate a mix of small unilamellar and multi-lamellar vesicles. The suspension was stored in small aliquots at -18 °C. Before each experiment, 5 µL of the liposome solution was deposited onto a glass cover slip, dried under vacuum at room temperature during 30 min, and rehydrated with 200 µL of PBS. The lipid film reorganized into lipid blobs on which giant liposomes (10-50 µm diameter) swell (15 min-duration process). The buffer solution containing GUVs and blobs was transferred using a 1000 µL pipette to a poly-L-lysine coated coverslip that was placed into a chamber for observations (Ludin Chamber Type 1). When necessary, the volume was increased to 1400 µL with Tris-phosphate buffer to allow a washing of immobilized GUVs using a peristaltic pump. The

GUVs were stable for at least one hour in these conditions.

Two methods have been used to expose GUV membranes to NOX proteins. The first method consists of local micro-injections under microscope with micropipettes made from pulled glass capillaries (WPI, TW100-f4; capillary puller Narishige, PC-10; Heat level of 80, 3 weights). The micropipettes were filled with the protein solutions at 300 nM protein using Eppendorf micro-loader tips, then mounted on the holder of a micro-injector (Eppendorf, Femtojet) and manipulated on the microscope platform with a piezo micromanipulator (Burleigh, PCS5000). To nebulize GUVs with protein solutions, the micropipette (few micron-diameter) was brought at about 10 µm distance from the GUV membrane and a flush of the solution was injected for a few tens of seconds in the membrane vicinity. The imaging of the process was performed in real-time. All the injected solutions contained 0.91 % ethanol. For the second method, 10 µL of GUVs suspension was gently mixed with PBS buffer (10-15 µL) containing trimera at a final concentration of 3 µM. With this method it was necessary to use a tenfold higher concentration of protein than with the previous method to perfectly visualize the interaction. Indeed, with the prior method, the GUV-protein interaction was visualized at the scale of a single GUV. In the second experiment, the solution of GUVs and the proteins were incubated together to image GUV-protein interaction on several GUVs. Finally, arachidonic acid (45 µM), when indicated, was added and gently mixed with the solution. The final volume was 30 µL. Imaging was performed after sedimentation of vesicles on the glass slide and steady-state of interactions was reached.

2.2.5 Confocal microscopy

The images were collected with a laser scanning confocal microscope (Leica SP5), using a 20-x objective (N.A. 0.6). Only one fluorophore was excited at a given time. Turquoise fluorescence was excited at 458 nm and detected with a photo-multiplier within a 471–623 nm window. Cherry fluorescence was excited at 543 nm and detected with a 557–709 nm window, and Alexa Fluor 647™ was excited at 633 nm and detected with a 643–795 nm window. To avoid excessive exposition and photo-bleaching of the sample, images were collected sequentially under non-continuous exposition. The acquired images were displayed using a pre-defined color look-up (LUT) table to highlight the fluorescence variations. The quantification was done with the software Leica LAS AF Lite and signal was considered as positive when the signal-to-noise ratio was greater than 1.5. The value of the signal was calculated by the mean of the fluorescence of the pixels along the membrane while the noise was the mean of the fluorescence of the pixels outside the GUV on the microscope field. Imaging of experiments with trimera was performed on a confocal microscope (Nikon) with a spinning-disk confocal system (Yokogawa CSU-X1-A1, Yokogawa Electric, Tokyo, Japan) associated with a Prime 95B sCMOS camera (Photometrics, Tucson, USA coupled with an ORCA-Flash 4.0 LT sCMOS camera (Hamamatsu, Japan).

2.3 In cellulo studies

2.3.1 Plasmid construction for PLB-985 cell transfection

The Citrine protein was obtained by introducing the Q69M mutation in the Yellow Fluorescent protein in the pEYFP-C1 plasmid (Clontech), the plasmid obtained was called pECitrine-C1. The cDNA of the four trimera were amplified by PCR using the following forward primer TTAAAGCTTCGATGGGGGACACCTTCATC except for ΔPX mutant TTAAAGCTTCGATGGACATCACCG and the following reverse primer TTAGGTACCTTCTTACAACAGCAGGC. The products were digested with KpnI and HindIII as well as the pECitrine-C1 plasmid and ligated. All the constructs were checked by sequencing (Beckman Genomics, UK) to confirm their identity.

2.3.2 Cell culture, differentiation and transfection

The human myeloid leukemia cell line PLB-985 WT and PLB-985 KO, with a targeted disruption of the gene coding for the catalytic subunit Nox2 of the NADPH oxidase [44], were grown in RPMI 1640 supplemented with 2 mM (4 %) L-Glutamine, 100 U/mL penicillin G, 100 µg/mL streptomycin, 250 ng/mL amphotericin B and 10 % of heat-inactivated fetal bovine serum. PLB-985 cells were differentiated into neutrophil-like cells by the addition of 1.25 % dimethyl sulfoxide (DMSO) for 6 days. Differentiated PLB cells were transiently transfected using the 4D-Nucleofector (Lonza, Switzerland) according to the manufacturer's protocol. For each protocol, 2×10^6 to 4×10^6 cells were transfected with 1 µg of vector and incubated in a culture medium without antibiotics using the SF Cell Line Kit (Lonza, Switzerland) and the EH-100 program. The PLB-985 WT cells were transfected with plasmids harboring the gene coding for the prototype trimera and the three mutant trimera (Tri-p47ΔPX, Tri-Rac1-PB2 and Tri-Rac1-PB6Q), while PLB-985 KO cell line was transfected only with a plasmid containing the gene coding for prototype trimera. The transfection was followed by 5 hours of incubation at 37 °C, then

the cells were counted, the transfection efficiency was measured and the cells were used for microscopy or ROS production measurements. The cell viability was evaluated by trypan blue coloration.

2.3.3 Flow-cytometry

Transfection efficiency was estimated by cytometry with a CyFlow flow cytometer (Partec/Sysmex) equipped with the Flomax software. For the measurement of transfection efficiency, Citrine was excited at 488 nm and detected with a 536/40 nm bandpass filter. Non-transfected cells were used for background calibration (see figure S1).

2.3.4 Microscopy

To visualize the cell cytoplasm, the transfected cells were incubated with 2 µM calcein blue AM (Invitrogen, France) for 10 min in Hank's Buffer Salt Solution (HBSS, Sigma), washed twice and resuspended in HBSS. For confocal microscopy imaging, cells were seeded on µ-Slide 8 well glass bottom chamber IBIDI and we used a spinning-disk confocal system (Yokogawa CSU-X1-A1, Yokogawa Electric, Tokyo, Japan). All the experiments were performed at 37 °C. Citrine was excited at 491 nm using a 0.3 s laser illumination and the fluorescence was detected with a 525/50 nm emission bandpass filter (Chroma, Olching, Germany). For confocal imaging, a series of 14-20 confocal z-planes (0.5 µm thickness each) were collected for each sample field.

2.3.5 Activity measurement

ROS production was measured using an L-012-based chemiluminescence assay. 2×105 transfected PLB-985 cells were plated in white polypropylene 96-well plates using a SynergyH1 plate reader (Biotek, USA). The assay was performed in an HBSS buffer at 37 °C. 100 µM L-012 (Wako Chemicals) and Horseradish Peroxidase (20 U/mL) were mixed and added to the wells and the record of the ROS production started. The ROS production was quantified by integrating the detected luminescence over time (5 hours) and the amount of luminescence of the PLB-985 KO transfected with the prototype trimera was subtracted. Each condition was performed in duplicate and three independent experiments have been realized. The measurements are expressed in relative luminescence units (RLU).

2.3.6 Image analyses and statistics

Image analysis was performed using Image J software. Graphpad prism8 software (GraphPad Software, USA) was used for the statistical analyses.

3. Results

3.1 Binding of separated cytosolic proteins on GUV with or without the activator AA

The binding experiments of the three proteins individually $p47^{phox}$, $p67^{phox}$ and Rac1Q61L to a phospholipid membrane were performed with giant unilamellar vesicles (see lipid composition table 1). The aim here was to evaluate the potency of combinations of these three proteins to bind to the membrane containing only phospholipids, without membrane proteins and notably in absence of cyt b_{558}. Proteins were labeled with different fluorophores displaying well-separated excitation and emission wavelength bands. Rac1Q61L was labeled at the N terminal position with Cherry fluorescent protein (FP) and annotated Cherry-Rac and $p67^{phox}$ with Turquoise FP, also at the N terminal position and annotated turq-p67. The Citrine fluorescent protein that was first fused with $p47^{phox}$ turned out to be sticky on glass and triggered protein aggregation in these conditions. Consequently, after some tests we chose the Alexa Fluor 647 maleimide to label cysteine residues of $p47^{phox}$, the labeled protein being annotated A-p47. In our conditions, the autofluorescence from the membrane lipids was found to be negligible. The visualization of the protein solutions under the microscope showed that the presence of arachidonic acid (AA) tended to aggregate the 47^{phox} and $p67^{phox}$ proteins in the micropipette and in the solution. This phenomenon has been described when the cell-free system was settled [45]. AA is known to activate the cytosolic proteins by inducing conformation changes at around 40 µM, which allow protein-lipid interactions and protein-protein interaction with cyt b_{558} leading to superoxide production [22].

Origin of membranes	Lipid composition
Neutrophil [18] [46] [16]	34.8% PC, 32.6 PE, 11.3% PS, 3.1 PI, 0.2% PA (18% nd) 30% PC, 28.4% PE, 10.3 PS 2.6% PI, 12.9% SM, 15.5% chol 30.2 % PC, 33.6 %PE, 10.7 %PS, 4.4%PI, nd PA, 0.9% PG, 19.3% SM
Macrophage [16]	33.6 % PC, 21.9% PE, 5.7% PS, 5.8% PI, 17.1% PA, 1% PG, 13.8% SM
Soybean lipid extract 45% ref 541602C (Avanti)	46 % PC, 22% PE, 18 % PI, 7 % PA, 7% unknown

Table 1: PPL composition of neutrophil membranes, macrophage membrane and soybean extract used in this paper. Abbreviations used: PC phosphatidyl choline, PE phosphatidyl ethanolamine, PS phosphatidyl serine, PI phosphatidyl inositol, PA phosphatidic acid, PG phosphatidyl glycerol, SM sphingomyelin, Chol Cholesterol, SPE soybean polar lipid extract, nd not determined.

The results presented in figure 1A show that, in absence of AA, when a mix of A-p47, turq-p67 and Cherry-Rac proteins was flushed toward the GUV, none of the three proteins bound on the vesicle membrane. Similarly, no

binding was observed when solutions containing one or two proteins without AA were used (data not shown). In the presence of arachidonic acid, no binding was observed when only turq-p67 or only Cherry-Rac, or both were present (fig 1C and 1D, left boxes). However, A-p47 was able to bind to the GUV membrane alone or in presence of Cherry-Rac (fig 1C and 1D, middle boxes). In these two cases, fluorescent proteins accumulation appeared with increased injection time toward the surface of the membrane, resulting in heterogeneous fluorescence and suggesting heterogeneous binding patterns of A-p47. In the presence of turq-p67, A-p47 effectively binds the membrane with a homogeneous distribution on its surface, as well as for $p67^{phox}$ (fig 1C, right box). When a mixture of the three proteins activated by arachidonic acid was used, a homogeneous and strong fluorescence at the membrane, stable over a few minutes, was easily seen.

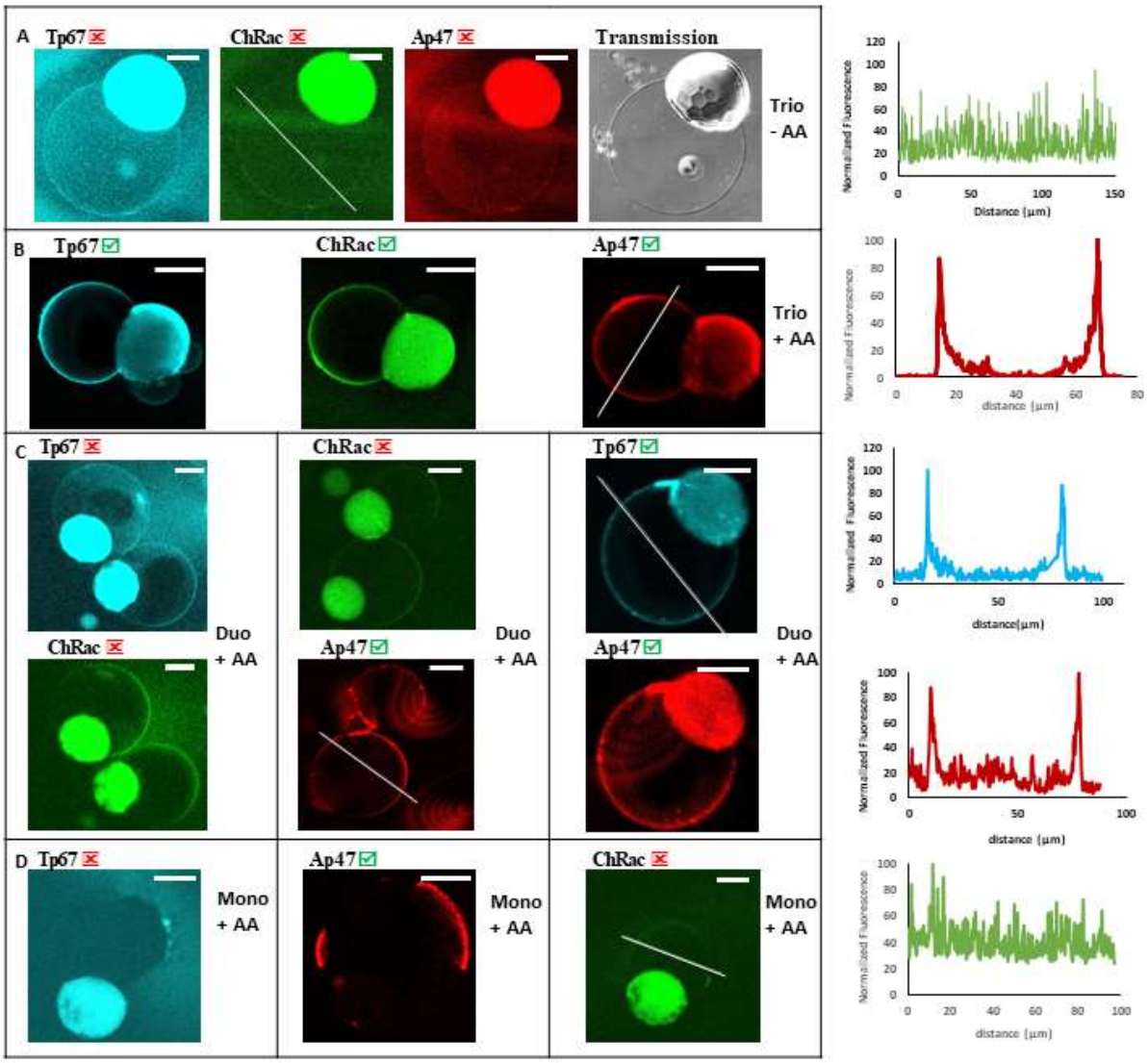

Figure 1: Representative laser-scanning confocal fluorescence microscopy images of cytosolic protein solutions binding on GUVs. *Cytosolic solutions containing :* ***(A,B),*** *a mix of turq-$p67^{phox}$ (annotated Tp67 in the Figure), Alexa-$p47^{phox}$ (annotated Ap47 in the Figure) and Cherry-Rac1Q61L (annotated ChRac in the Figure) proteins,* ***(A)*** *in absence or* ***(B)*** *in the presence of AA;* ***(C),*** *a mix of turq-$p67^{phox}$ and Cherry-Rac (on the left) or a mix of Cherry-Rac and Alexa-$p47^{phox}$ (in the middle) or a mix of turq-$p67^{phox}$ and Alexa-$p47^{phox}$ proteins (on the right), in the presence of AA;* ***(D)*** *a solution containing only turq-$p67^{phox}$ (on the left) or only Alexa-$p47^{phox}$ (in the middle) or only Cherry-Rac protein (on the right) in presence of AA, were flushed towards GUV. On the right, representative fluorescence intensity graph is shown of one of the fluorescent proteins along the line drawn in the images. The concentration of each protein was 300 nM, and of AA was 50 µM. The GUVs have been prepared as described in material and methods section 2.2.4. The white scale bars correspond to 25 µm. The excitation wavelengths of the Turquoise FP, Cherry FP and Alexa 647 were 458 nm, 543 m and 633 nm, respectively, with emission wavelengths 468-795 nm, 553-795 nm and 643-795 nm, respectively. All the GUV observed in these experiments are associated with a lipid reservoir where proteins tend to accumulate and where lipid unspecific autofluorescence may be seen.*

These results also showed that the binding of the three proteins mixed together was possible on a membrane made solely of phospholipids, in the presence of AA. This suggests that the presence of cyt b_{558} embedded into the membrane was not required for this interaction. Moreover, A-p47 was the only protein to be able to bind to the membrane on its own and was required to trigger the membrane binding of turq-p67 and Cherry-Rac. This set of experiments showed the importance of protein-protein interactions involving $p47^{phox}$ in the formation and stability of the p47-p67-Rac heterotrimer at the membrane. These experiments also enhanced the importance of AA as an activator of these proteins. However, the stoichiometry of the formed complex is unknown. To partially solve this issue, we have used in the following the chimeric proteins called trimera described above.

3.2 Binding of trimera on GUVs with or without activator

The results on isolated proteins showed that they all bind to the GUV membranes when they translocate together in presence of AA. The membrane binding of these proteins occurs through interactions between some phospholipids (PA, PS, PI3,4P2) and the two lipid-binding sites, PX for $p47^{phox}$ and PB for Rac [12]. To investigate the importance of these lipid-binding sites in modulating the binding of the cytosolic proteins, we used four different trimeras fused to a green fluorescent protein (GFP), constructed in Pr. E. Pick's laboratory [39]. The trimera prototype was designed to preserve all essential interactions of the cytosolic proteins necessary to form the active state of the enzyme: *i.e.* interactions between $p67^{phox}$ and Rac, $p67^{phox}$ and Nox2, $p47^{phox}$ and $p22^{phox}$, and importantly for this study Rac and $p47^{phox}$ with lipids [31, 39]. This chimeric protein ensures the formation of NADPH oxidase complex with the right stoichiometry in cytosolic proteins: 1:1:1 for $p47^{phox}$, $p67^{phox}$ and Rac. It has also been found to be much more stable than the separated proteins that dissociate faster after dilution [31]. Three variants of the prototype were used in this work: $p47^{phox}$ ΔPX, Rac1-PB2 and Rac1-PB6Q trimeras. $p47^{phox}$ ΔPX trimera was deleted for the phospholipid interacting domain PX of $p47^{phox}$. Tri-Rac1-PB2 and Tri-Rac1-PB6Q were mutated in the phospholipid interacting polybasic domain of Rac1, leading to a loss of the six charges (Tri-Rac1-PB6Q) or the exchange of the polybasic region of Rac1 with the one of Rac2 (Tri-Rac1-PB2) (see figure S2). It has been shown that Rac1 and Rac2 bind differently to membranes, depending on the variation in PB composition and lipid composition, leading to different subcellular localization [47].

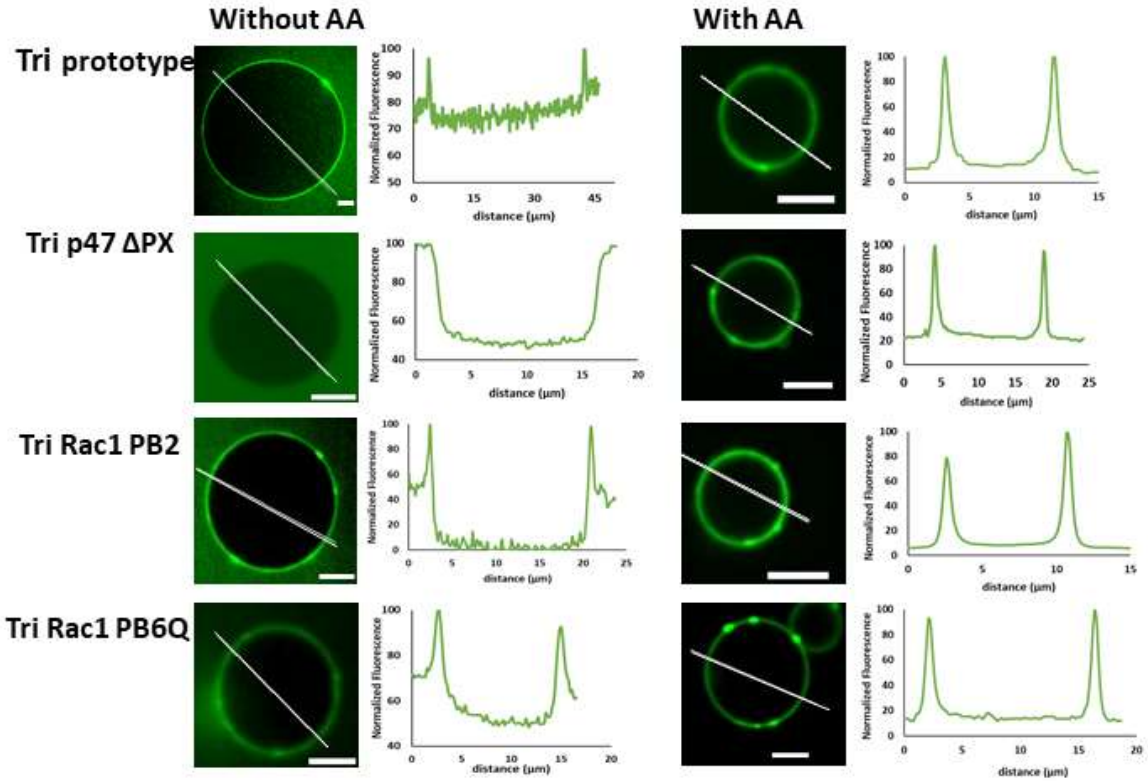

Figure 2: Spinning disk confocal fluorescence microscopy images of prototype or mutated GFP trimera binding to giant liposomes membranes. *GUVs were incubated with a prototype or mutated GFP trimera solution as indicated on the top of the image and as described in material and methods section 2.2.4, in absence or in presence of 45 µM AA. Representative image of each condition is shown and fluorescence intensity graph of the trimera along the line drawn in the images. The concentration of GFP-trimera was 3 µM. The white bars correspond to 5 µm.*

As seen in figure 2, the prototype was able to bind on the GUV membrane in absence of AA, as well as Tri-Rac1-PB2 and Tri-Rac1-PB6Q but the $p47^{phox}$ ΔPX mutant did not. This result suggests that the prototype, Tri-Rac1-PB2 and Tri-Rac1-PB6Q take a conformation that makes the PX domain of $p47^{phox}$ accessible for interacting with lipids. When the $p47^{phox}$ PX domain was missing, no trimera was able to attach to the GUVs strengthening the suggestion that $p47^{phox}$ through its PX binding domain constitutes a driver of the trimera to bind on this membrane. The decrease of charges in the PB region had little effect since the trimera were still tightly bound through the PX domain.
In the presence of 45 µM AA, (figure 2) no significant difference was observed on the fluorescence signal on the GUV between the prototype and the mutants. All variants could bind on vesicle membranes showing that both domains could tightly bind to the model membrane. Furthermore, as with the separated proteins, the presence of AA generated the formation of fluorescent aggregates that could consist of a mixture of arachidonic acid micelles and trimera, or precipitated trimera. An increase in AA concentration (100-160 µM) decreased the fluorescence level on the GUV membrane and increased the amount of aggregates (data not shown).

3.3 Binding of the trimera prototype and mutants on unstimulated PLB-985 cell membranes

Next, the localization of the four trimera constructions was studied in myeloid PLB-985 cells differentiated into neutrophil-like cells. The PLB-985 KO deleted for the Nox2 gene has also been used to distinguish between an effect of the mutation on the interaction with phospholipids and a decrease in their binding abilities to cyt b_{558}. The confocal microscopy images (figure 3) show that, as previously observed in COS7 cells [48], the prototype GFP-trimera was almost entirely localized on the plasma membrane regardless of whether Nox2 was present (top line and bottom line, figure 3), whereas the localization of the three mutated citrine-trimera was more dispersed. The use of calcein blue, which labels the cytoplasm and the nucleus of cells, allowed us to draw a ratio between trimera and calcein fluorescence to highlight the membrane localization of the trimeras. The Tri-p47ΔPX variant was mainly localized to the plasma membrane, while the Tri-Rac1-PB2 and the Tri-Rac1-PB6Q were mainly localized in the cytoplasm. The trimeras were not detected in the nucleus.

3.4 In vitro NADPH oxidase activation by GFP-trimeras

The NADPH oxidase complex needs to be activated *in vitro* and *in vivo* for its assembly and for superoxide anion production. To better determine the influence of the protein-lipid interactions on the formation of active NADPH oxidase complex, the GFP-trimera prototype and the mutants were used in a cell-free assay to activate Nox2 in plasma membrane fractions of human neutrophils. Thus, AA-dependence experiments have been performed in the presence of 300 nM trimera, a protein concentration similar to those used with separated cytosolic proteins [27, 42]. As previously described with macrophage plasma membranes [31], the trimera prototype and mutants still required the addition of amphiphilic molecules such as arachidonic acid to activate cyt b_{558} (figure 4). The arachidonic acid-dependence of the NADPH oxidase activity with the prototype GFP-trimera followed the typical bell-shaped curve generally observed with the cytosolic proteins. It shows an increase of the enzyme activity from 0 to about 40 µM AA, followed by a decrease of the activity above 40 µM AA that is likely due to protein denaturation, complex dissociation or membrane disruption. The optimal concentration of AA, about 40 µM, leading to the maximal activity was also found close to that obtained with the separated cytosolic proteins. The mutant Tri-p47ΔPX showed slightly lower activity whereas the two mutants Tri-Rac1-PB2 and Tri-Rac1-PB6Q displayed a big decrease in activity and greater sensitivity to AA deactivation. This higher decay could be due to a lower stability of the complex. The same experiment has been performed using membrane fractions prepared from PLB-985 cells. As with neutrophil membranes, we obtained an activation and deactivation phase as a function of the AA concentration with an optimal concentration of about 30 µM (figure S3). However, two observations were different: first, a substantial activity (20-40 % of the optimal value) was observed when trimeras were added to PLB cell membrane fractions in the absence of AA; this lack of AA requirement suggests that trimeras *per se* can partly bind and activate cyt b_{558}. Secondly, the effect of the mutations of the two lipid binding sites was different since the complex of Nox2 with $p47^{phox}$ ΔPX trimera showed low activity compared to the prototype whereas the Rac1-PB2 trimera lead to activities similar to the prototype. To determine if this general decrease of activity of the GFP-trimera mutants relative to the prototype may be explained by a decrease of affinity for cyt b588, a dependence of activity as a function of GFP-trimera variants concentration was studied. The results reported in figure 5 show that the three modifications have weakened the capacities of the protein to bind on Nox2 since the EC50 of the mutants were increased by 5-6-fold compared to the prototype. The mutants kept similar abilities to activate the enzyme except for Rac1-PB6Q, which showed a 20 % decrease in V_{max}.

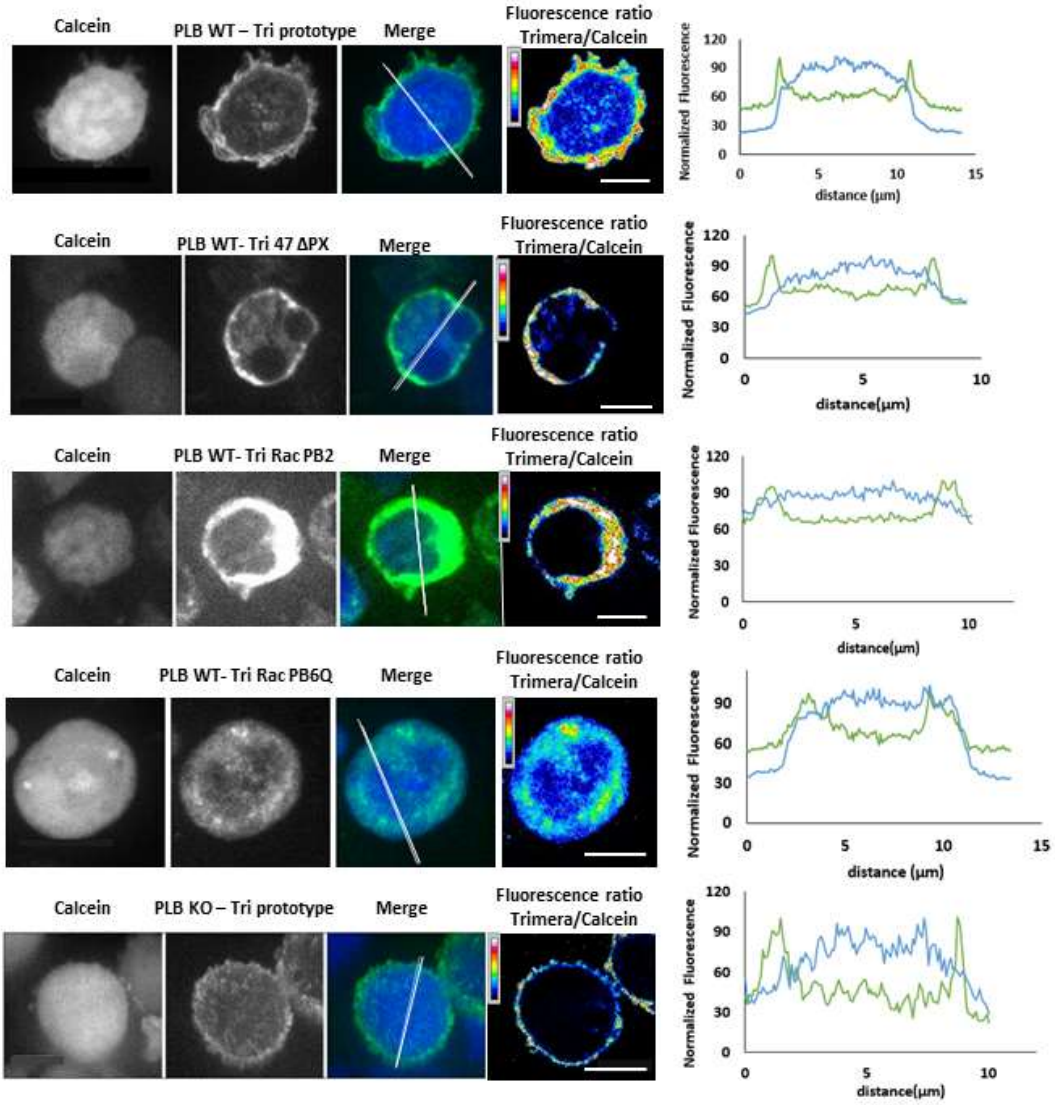

Figure 3 Spinning-disk confocal fluorescence microscopy images of PLB-985 (WT and KO) cells expressing Citrine-trimera prototype and mutants. *Representative images are shown for each condition. From left to right: images of calcein blue staining (cytosol and nucleus), Citrine-trimera, merge images of both and fluorescence ratio Citrine/calcein. The graph on the right shows the fluorescence intensities of the trimera and the calcein blue along the line drawn in the merge images. In the merge images, calcein staining is in blue and Citrine-trimera constructs fluorescence is in green levels. White scale bars equal 5 µm.*

3.5 Superoxide anion production measurements of PLB-985 cell expressing Citrine-trimera prototype and mutants

The four trimera constructions fused with the Citrine FP have been expressed in PLB-985 cells differentiated in neutrophil-like cells. As seen in figure 6A, the transfected level of the trimera was greater than 50 % and very close for the four proteins indicating that similar levels of Citrine-trimera were expressed in all transfected cells. As a reminder, in the resting state, the endogenous NADPH oxidase proteins are in a non-assembled inactive state, therefore the non-transfected cells do not produce superoxide anion. With the transfected cells, a constitutive superoxide anion production was measurable in the resting state (Figure 6B and C). The superoxide anion production in resting PLB-985 cells expressing Citrine-trimera, was in the same order as the one measured with PLB-985 cells activated with PMA (figure 6C and D) and due to endogenous phox proteins. These results show that the Citrine-trimera constructs were able to activate constitutively the NADPH oxidase enzyme in PLB-985 cells, in an equivalent manner to the endogenous cytosolic proteins but without the need for an activator. This data agrees with our previous results obtained with COS7 cells [48] and with the observation of Citrine-trimeras constitutively located at the plasma membrane as presented in Figure 3. Besides, a strong decrease in superoxide anion production was observed for the two Citrine-trimera variants involving mutations in the PB region of Rac1, which also correlated with their main localization in the cytoplasm. The continual high level of ROS production causes acidification of the intracellular pH, triggers apoptosis and leads to local peroxidation of lipids in the membrane. These local damages are correlated to a distribution in cluster of Nox2 and trimera [38].

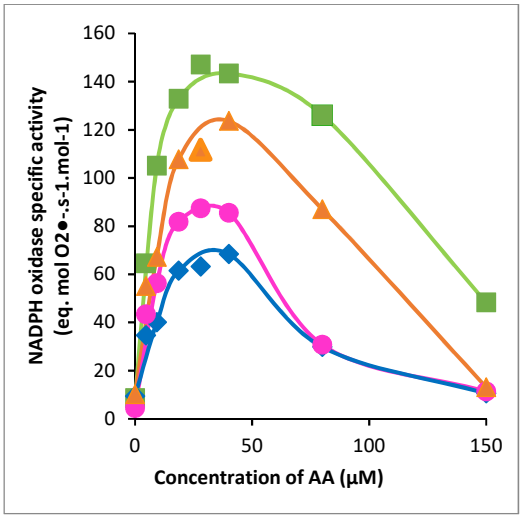

***Figure 4*: AA-dependence of NADPH oxidase activation by GFP-trimeras in cell-free assays.** *The capacity of GFP-trimera prototype and mutants to activate the NADPH oxidase in the presence of arachidonic acid was assayed by mixing neutrophil MF at a concentration equivalent to 4 nM cytochrome b_{558}, with 300 nM of the following trimera: prototype trimera (■); p47^{phox} ΔPX trimera (▲); Rac1-PB2 trimera (●); Rac1-PB6Q trimera (◆) and an increasing concentration of AA. Superoxide anion production was initiated by the addition of NADPH (200 µM). Measurements were performed as described in the Material and Methods section 2.2.3. Each point is the mean of the results obtained from 3 different membrane fractions. The standard error corresponds to about 10 % of rate values.*

A

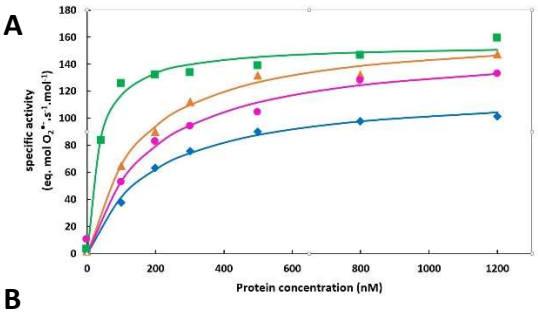

B

Trimera	V_{max} (eq. mol $O_2^{\bullet-}.s^{-1}.mol^{-1}$)	EC_{50} (nM)
Prototype	154 ± 4.28	31.9 ± 5.81
P47 ΔPX	165 ± 5.02	151 ± 16.7
Rac1-PB2	154 ± 8.3	187± 33.5
Rac1-PB6Q	121 ± 3.71	188 ± 19.1

Figure 5 Kinetic parameters for GFP-trimera prototype and mutants using Michaelis-Menten equation in presence of AA. (A): *Activity in function of trimera concentration. The assay mixtures consisted of trimera (prototype trimera (■); GFP-trimera p47^{phox} ΔPX (▲); GFP-trimera Rac1-PB2 (●); GFP-trimera Rac1-PB6Q (◆)) at varying concentrations (from 0 to 1200 nM) and membrane fractions of human neutrophils (4 nM cyt b_{558}) to which were added 40 µM AA. The superoxide formation was measured as indicated in Materials and Methods. (B): The EC_{50} values and Vmax values are an average of three independent measurements ± SD.*

4 Discussion

4.1 Arachidonic acid effect on the translocation of isolated cytosolic proteins and trimera on membrane in vitro

In dormant cells, 100 % of the three cytosolic proteins p47^{phox}, p67^{phox} and Rac are found in the cytosol [19-21, 49]. These proteins must undergo posttranslational modifications to bind to the membranes (figure 7). The experiment presented in figure 1 shows the cytosolic proteins p47^{phox}, p67^{phox} and Rac1Q61L interacting with GUV membranes. These model membranes are made of a natural polar lipid mix (table 1). *In vitro,* arachidonic acid triggers an opening of the protein structures, thus they will be able to interact with phospholipids and to other proteins of the complex [50]. We observed that the cytosolic proteins p47^{phox}, p67^{phox} and Rac1Q61L bind to the membrane only in the presence of AA, especially when the three proteins were present together. This result confirms that the p47^{phox} and p67^{phox} cytosolic proteins must adopt an open conformation to interact with a membrane. The removal of the autoinhibitory domains of p47^{phox}, the PB1 and SH3 domains of p67^{phox} and their fusion with Rac1Q61L gives to the prototype trimera the ability to bind to the model membrane in absence of AA. This fused protein is also capable of binding to the plasma membranes of PLB-985 and COS7 cells and to constitutively produce ROS [48] showing that the trimera is expressed in the open conformation *in vitro* and *in vivo*.

It is important to note that these translocations to the membrane (with GUVs but also in PLB 985 and COS7 cells) occur in the absence of cyt b_{558}. Our experiment leads to the surprising conclusion that Nox2 is not mandatory for membrane binding of cytosolic proteins p47^{phox}, p67^{phox} and Rac1Q61L. The binding of Rac to the membrane in the absence of Nox2 has been described previously [19, 51], which is not the case for p47^{phox}[20]. The binding of the cytosolic proteins may suggest that in activated phagocyte cells, the cytosolic proteins bind to the phospholipids before the assembly on cyt b_{558}. This assembly would then stabilize the binding of each protein on the membrane. This hypothesis may be linked to the observation in the cell-free assay that the cytosolic proteins must be incubated quickly with membrane fractions and in presence of arachidonic acid for a fully functional NADPH oxidase. Then, the assembled protein complex to the membrane fractions is stable for at least 90 minutes without activity loss at 25 °C [42]. The fusion of these three proteins would thus render this lipid binding step more stable than when compared to the isolated and full-length proteins.

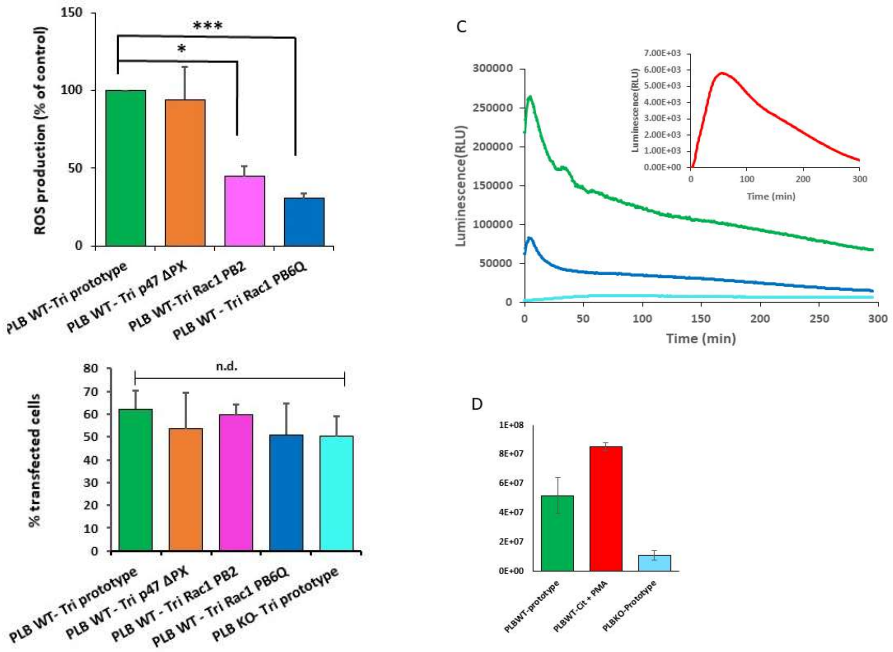

Figure 6 Measurement of ROS production in PLB-985 cells expressing Citrine-trimera prototype and mutants. ***(A)*** *Transfection rate of PLB-985 cells for the Citrine-trimera prototype and mutants measured by cytometry as described in the Material and Methods section and in figure S1.* ***(B)*** *Production of ROS using L-012 based chemiluminescence assay. The ROS production was quantified as integrated luminescence over time (5 hours, at 37 ° C) and the amount of integrated luminescence of the PLB-985 KO transfected with the prototype trimera was subtracted. The zero time corresponds to the addition of L-012. The results were normalized to the value found with the prototype. Each condition was performed in duplicate and three independent experiments have been realised. Statistical analysis comes from a Kruskal-Wallis test followed for* ***B*** *by a Dunn's test for multiple comparisons. * and *** correspond to a p value < 0.05 and < 0.005 respectively.* ***(C)*** *Example of ROS production as function of time in PLB WT cells expressing Citrine-trimera prototype (green) or Citrine-trimera Rac1 PB6Q (dark blue) and in PLB KO cells expressing Citrine-trimera prototype (light blue). In the insert caption: kinetics of ROS production in PLB WT cells expressing Citrine protein activated by 200 nM PMA.* ***(D)*** *Same as B except that the values were not normalized. The PLB WT Citrine cells were activated by 200 nM PMA. The zero time corresponds to the addition of PMA.*

4.2 Beneficial effect of the presence of the cytosolic partners for the translocation to membranes of p47^{phox}, p67^{phox} and Rac

It has been demonstrated that p67^{phox} needs the formation of the p47^{phox}-p67^{phox} dimer to migrate to a membrane. This was attributed to a lack of a lipid binding site in p67^{phox} [20]. The results presented in figures 1B and 1C, are in agreement with this observation since p67^{phox} alone could not bind to GUV. As soon as p47^{phox} was present, p67^{phox} was found at the membrane surface. The same situation was observed for Rac. Thus, Rac and p67^{phox} are stabilized by p47^{phox} on this membrane.

On the other hand, p47^{phox} was always found at the membrane when activated by arachidonic acid, but appeared as possible large oligomerization patches at the surface of the membrane when alone. This was no longer the case when p47^{phox} was associated with p67^{phox} since the fluorescence signal appeared homogenous. Therefore, the interaction with p67^{phox} can be considered beneficial for a homogeneous membrane binding of p47^{phox}. A similar but less pronounced observation was seen in presence of Rac that was not significantly found on the membrane in presence of p47^{phox}. In cells, Rac has been found to translocate independently (it does not bind to p47^{phox}-p67^{phox} in the cytosol) [19] but simultaneously to p47^{phox}-p67^{phox} heterodimer translocation [21]. The lack of binding of Rac1 alone on GUV and the formation of oligomerization in absence of p67^{phox} may suggest a slight interaction between p47^{phox} and Rac1 that may not exist in physiological conditions. Concomitant translocation of the three proteins avoided the formation of oligomerization and helped Rac1 to bind more firmly through its interaction with p67^{phox}. Since Rac1Q61L is produced in *E. coli* which lacks the prenylation machinery, a second possibility is that the absence of prenylation on Cys189 *in vitro* partly impairs the binding capacity of Rac compared to *in vivo* [39]. This renders Rac1 binding more dependent on the presence of p67^{phox} and p47^{phox} *in vitro*. To summarize, the presence of the three proteins in an active state stabilizes them at the membrane since a homogeneous and rather good fluorescence signal-to-noise ratio was observed on the surface of GUVs in this case. This phenomenon was also observed for kinetic measurements by the high increase of affinity of each cytosolic protein for the Nox2 membrane protein in the function of the two other proteins concentration [26, 27] and the previous observation showing the need for concomitant binding of the three cytosolic proteins on cyt b_{558} for the formation of a fully activated NADPH oxidase complex [27].

4.3 Comparison of prototype trimera interaction with neutrophil, PLB-985 cells and GUV membranes

Since the *in vivo* and *in vitro* translocation of the three isolated proteins p47^{phox}, p67^{phox} and Rac occurs simultaneously and in a very dependent way, the use of a fused p47^{phox}-p67^{phox}-Rac protein proved to be very suitable to test different membranes. Several publications have shown that cytosolic proteins do not bind to all types of membranes even in their activated state. These membranes must contain specific phospholipid (PPL) compositions including anionic PPL providing enough negative charge content [31, 36, 37, 39]. The results presented in this paper show that the prototype trimera bind differently on the membrane of neutrophils, PLB-985 cells and GUV. *In vitro*, AA is required to activate trimeras for superoxide production by the MF of neutrophils, macrophages [31, 39] and PLB-985. Thus, the PPL composition of the plasma membrane from resting neutrophils does not allow the binding of the trimera. A slight activation in absence of AA has been found

with MF of PLB-985 cells (figure S3), suggesting a difference in membrane composition. On the other hand, *in vivo*, the trimera interacted extremely well with the plasma membrane of resting transfected PLB-985 (this work) or COS7 cells [48]. This difference in trimera membrane binding ability, between *in vitro* and *in vivo* conditions, could be due to the prenylation of Rac, a posttranslational modification that occurs in cells and not in *in vitro* systems that has been found to greatly favor the binding of the trimera on macrophage MF [39]. The binding of the prototype trimera observed in absence of AA on GUV (figure 2) and on macrophage membrane vesicles enriched with anionic phospholipid [31] suggests that the PPL composition of GUVs from soybean polar lipid extract constituted a favorable platform for trimera interaction, mainly with its PX domain. In terms of charges, the membranes of neutrophils, macrophages and GUVs have about 15 %, 30 % and 25 % (w:w) of negatively charged PPL, respectively (table 1). Thus, neutrophil and macrophage membranes seem to have globally enough charges for trimera binding. However, their repartition is known to be asymmetric between the inner and outer leaflet and different for the plasma membrane, the phagosome and endosomes. In terms of membrane phospholipid composition, the major differences between neutrophils, macrophages and GUVs are the percentage of phosphatidic acid (PA), a PPL important for the binding of the PX domain. This is absent in neutrophils but present in macrophages (17 %). Phosphatidylinositol (PI) is present at 18 % in GUVs compared to 3-4 % and 5.8 % in neutrophils and macrophages respectively. Phosphatidylserine (PS) is totally absent in these GUV membranes whereas it is highly present in the inner leaflet of neutrophils. A well-defined PPL composition of the cell studied seems important in resting and activated state, for the plasma and phagosome membrane. Then a screening of liposomes with compositions close to the one determined with and without membrane proteins would be necessary to better understand the interactions of the isolated proteins. Nevertheless, the PPL composition comparison performed herein suggests that AA acts mainly by modifying the close environment of Nox2, thus hindering the positive patches of the membrane proteins. It could also act by inducing a conformation change of the trimera for a better binding rather than through an increase of the negative charge amount at the surface of these membranes.

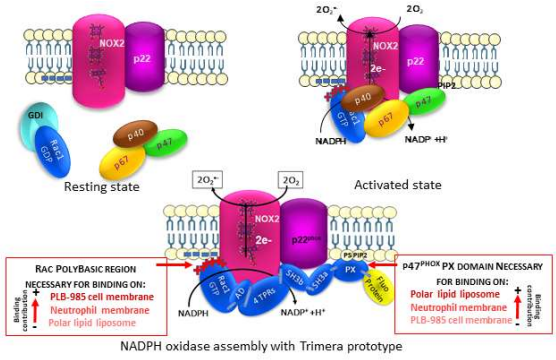

Figure 7: Scheme of NADPH oxidase enzyme in resting and activated state of cells, and in presence of prototype trimera.

4.4 Role of the PB anchor on the interaction of the trimera on membrane and Nox2; Rac1 versus Rac2 story

The results obtained on the trimera binding properties show that the prototype has sufficiently similar characteristics compared to the active form of the cytosolic proteins. No supplementary activation was necessary for the prototype trimera to bind on GUV and PLB-985 cells but also for superoxide anion production *in cellulo*. In the mutant Tri-Rac1-PB6Q, the loss of Rac1 polybasic region induced *in cellulo* (figure 6) and *in vitro* (figure 5) a decrease in ROS production. This decreased activity is accompanied by a strong decrease of the membrane binding on membrane fractions from neutrophils (an increase of EC_{50} of the trimera for Nox2) or on PLB-985 cells (figure 3). A similar effect of the Rac1-PB6Q trimera was described on macrophage membranes [31]. Thus, the interaction between the PB region of Rac1 and the membranes plays a large part in the binding of the trimera in these different cells. However, we observed that this mutated trimera can bind to GUV membranes in the absence of cyt b_{558} and AA. This might be attributed to the particular PPL composition of soybean GUVs. The PB region was not as essential for the trimera binding relative to the PX domain as with the other membranes tested. Berdichevsky et al [31] have shown the requirement of anionic phospholipids (PA, PG, PS or PI) for a trimera binding on liposomes. From our work, we conclude that the anionic PPLs present in resting macrophages, neutrophils or PLB-985 cells (see table 1) are not sufficient for the binding of this mutated trimera through the remaining PX domain, but those present on GUV membranes are adequate enough.

Rac2 expression is restricted to hematopoietic cells and is predominant in neutrophils (75-90 %) [52] whereas Rac1 is ubiquitously expressed. It has been shown that the PB region is responsible for the isoform-specific targeting mechanism of Rac. In neutrophils, Rac2 is involved in superoxide production at the phagosomal membrane whereas Rac1 accumulates at the plasma membrane which is more negatively charged [37, 53, 54]. In macrophages and monocytes, Rac1 is the isoform most implicated in superoxide production during phagocytosis. In Raw 264.7 macrophages, it has been found that, in resting state, Rac1-RhoGDI was localized in the cytoplasm and nucleus and Rac2-RhoGDI in the cytoplasm and Golgi [30]. Then, during FC□R mediated phagocytosis Rac1 accumulates strongly at the membrane in opposite to Rac2 and this difference was due to the PB region. In the PLB-985, neither the trimera harboring the PB of Rac1 (prototype) nor of Rac2 (Tri-Rac1 PB2) seems to accumulate in the nucleus. This is probably due to the size of the trimera or the presence of the other domains. We expected that the mutant Tri-Rac1-PB2 used in our work would display the phospholipid binding characteristics of Rac2. Indeed, this mutated trimera has kept more capacities to activate cyt b_{558} embedded in neutrophil membranes than it did from macrophages. This mutated trimera binds moderately on the PLB-985 plasma membrane and showed a 55 % decrease in activity, suggesting that the role of the PB region is of lower importance compared to neutrophils and macrophages. Effectively, Rac2 participates in phagosomal ROS production in these cells [36].

4.5 Role of the PX anchor on the interaction of the trimera on membrane and Nox2

It is well described that the target of $p47^{phox}$ is mainly the plasma membrane of activated cells. We observed a 5-fold increase of EC_{50} of Tri-p47ΔPX for neutrophil cyt b_{558} compared to the prototype trimera, a good binding on the resting PLB-985 cell plasma membrane and no binding on the GUV membrane in absence of AA. A 2-fold increase of EC_{50} for macrophage membrane had also been seen. These results show that the binding of the $p47^{phox}$ PX domain depends on the membranes, with a stronger participation in trimera binding on neutrophils than macrophage membranes [31]. This may be due to the lower concentration of negative charges in neutrophil than in macrophage membranes. The very little binding of Tri-Rac1-PB6Q on the PLB-985 plasma membrane suggests that the remaining PPL binding site, the PX domain, plays a small role in the binding affinity of the trimera on this plasma membrane. In the opposite case, the deletion of the PX domain, and not the mutation of the PB region, prevents the binding of the trimera on GUV membranes suggesting an important role of the PX domain in this PPL composition.

4.6 Conclusion

In agreement with previous statements, our results show that the lipid-protein interactions are crucial for the assembly of the NADPH oxidase proteins. The presence of prenyl on Rac is important but not sufficient for a good membrane interaction, the two other membrane anchors (PB and PX) participate largely in maintaining the trimera on the plasma membrane because they have a strong involvement in the EC_{50} values. Previously we had shown that the loss of interaction between $p67^{phox}$ and $p47^{phox}$ (deletion of the PRR of $p47^{phox}$) had little impact on $p67^{phox}$ binding for Nox2 [27]. The N-$p47^{phox}$ (aa 1-286) and N-$p67^{phox}$ (1-212) proteins also retained good abilities to form active NADPH oxidase [55, 56]. Moreover, the fusion of the three proteins has a high impact on the stability of the NADPH oxidase complex formed [31, 57]. The lower stability of the enzyme with the isolated cytosolic proteins is probably physiologically necessary for the ending of the anion superoxide production, but also continuous translocation [36, 58].

The three isolated proteins mixed together were all able to bind to the model phospholipid membrane in presence of AA and thus cyt b_{558} was not always required for this interaction. Moreover, $p47^{phox}$ was the sole protein able to bind to the membrane on its own, and is required to trigger the membrane binding of $p67^{phox}$ and non-prenylated Rac. This first set of experiments showed the importance of protein - protein interactions in the formation and the stability of the heterotrimer of the individual $p47^{phox}$, $p67^{phox}$ and Rac1Q61L on the surface of a membrane. Finally, it suggests that the phospholipid composition of GUVs has interesting features, in terms of charge and head groups (such as PA, PS and PI) or chain length for PPLs, for the isolated cytosolic protein assembly. This would then be a good starting point to study Nox2 assembly on plasma and phagosomal membranes. The relatively small differences in the PPL composition of neutrophil, macrophage plasma membrane and soybean polar lipid extract (table 1) suggest that the PPL content necessary for a good binding for both PB and PX domains and the cyt b_{558} is probably very precise. It suggests that small variations could trigger the binding and dissociation of the cytosolic proteins and thus control the NADPH oxidase enzyme activity.

Acknowledgement- We are very grateful to Pr. E. Pick for providing trimeras expression plasmid and for helpful discussion, Paul Machillot for the construction of expression plasmids of cytosolic proteins, Elodie Hudik for technical help on cytometry experiments and the Academic Writing Center for proof-reading service. The present work has benefited from Imagerie-Gif core facility, supported by l'Agence Nationale de la Recherche (ANR-11-EQPX-0029/Morphoscope, ANR-10-INBS-04/FranceBioImaging; ANR-11-IDEX-0003-02/ Saclay Plant Sciences).

Funding This work was supported by the Joint PhD Program of University Paris-Saclay as part of the « Investissements d'Avenir » program [grant number ANR-11-IDEX-003].

References

1. Vermot, A., Petit-Hartlein, I., Smith, S. M. E. & Fieschi, F. (2021) NADPH Oxidases (NOX): An Overview from Discovery, Molecular Mechanisms to Physiology and Pathology, *Antioxidants-Basel.* **10**, 890-945.
2. Groemping, Y. & Rittinger, K. (2005) Activation and assembly of the NADPH oxidase: a structural perspective, *Biochem J.* **386**, 401-16.
3. Sumimoto, H. (2008) Structure, regulation and evolution of Nox-family NADPH oxidases that produce reactive oxygen species, *FEBS J.* **275**, 3249-77.
4. El-Benna, J., Dang, P. M., Gougerot-Pocidalo, M. A., Marie, J. C. & Braut-Boucher, F. (2009) p47phox, the phagocyte NADPH oxidase/NOX2 organizer: structure, phosphorylation and implication in diseases, *Exp Mol Med.* **41**, 217-25.
5. Faust, L. R., el Benna, J., Babior, B. M. & Chanock, S. J. (1995) The phosphorylation targets of p47phox, a subunit of the respiratory burst oxidase. Functions of the individual target serines as evaluated by site-directed mutagenesis, *J Clin Invest.* **96**, 1499-505.
6. Forbes, L. V., Truong, O., Wientjes, F. B., Moss, S. J. & Segal, A. W. (1999) The major phosphorylation site of the NADPH oxidase component p67phox is Thr233, *Biochem J.* **338 (Pt 1)**, 99-105.
7. Belambri, S. A., Rolas, L., Raad, H., Hurtado-Nedelec, M., Dang, P. M. & El-Benna, J. (2018) NADPH oxidase activation in neutrophils: Role of the phosphorylation of its subunits, *Eur J Clin Invest.* **48 Suppl 2**, e12951.
8. Pick, E. (2014) Role of the Rho GTPase Rac in the activation of the phagocyte NADPH oxidase: outsourcing a key task, *Small GTPases.* **5**, e27952.
9. Di-Poi, N., Faure, J., Grizot, S., Molnar, G., Pick, E. & Dagher, M. C. (2001) Mechanism of NADPH oxidase activation by the Rac/Rho-GDI complex, *Biochemistry.* **40**, 10014-22.
10. Marcoux, J., Man, P., Petit-Haertlein, I., Vives, C., Forest, E. & Fieschi, F. (2010) p47phox molecular activation for assembly of the neutrophil NADPH oxidase complex, *The Journal of biological chemistry.* **285**, 28980-90.
11. Lewis, E. M., Sergeant, S., Ledford, B., Stull, N., Dinauer, M. C. & McPhail, L. C. (2010) Phosphorylation of p22phox on threonine 147 enhances NADPH oxidase activity by promoting p47phox binding, *J Biol Chem.* **285**, 2959-67.
12. Ago, T., Kuribayashi, F., Hiroaki, H., Takeya, R., Ito, T., Kohda, D. & Sumimoto, H. (2003) Phosphorylation of p47(phox) directs phox homology domain from SH3 domain toward

phosphoinositides, leading to phagocyte NADPH oxidase activation, *P Natl Acad Sci USA.* **100**, 4474-4479.
13. Marcoux, J., Man, P., Castellan, M., Vives, C., Forest, E. & Fieschi, F. (2009) Conformational changes in p47(phox) upon activation highlighted by mass spectrometry coupled to hydrogen/deuterium exchange and limited proteolysis, *FEBS Lett.* **583**, 835-40.
14. Jeschke, A. & Haas, A. (2016) Deciphering the roles of phosphoinositide lipids in phagolysosome biogenesis, *Commun Integr Biol.* **9**, e1174798.
15. Song, Z., Hudik, E., Le Bars, R., Roux, B., Dang, P. M., El Benna, J., Nusse, O. & Dupre-Crochet, S. (2020) Class I phosphoinositide 3-kinases control sustained NADPH oxidase activation in adherent neutrophils, *Biochem Pharmacol.* **178**, 114088.
16. Mason, R. J., Stossel, T. P. & Vaughan, M. (1972) Lipids of alveolar macrophages, polymorphonuclear leukocytes, and their phagocytic vesicles, *J Clin Invest.* **51**, 2399-407.
17. Serhan, C. N., Broekman, M. J., Korchak, H. M., Marcus, A. J. & Weissmann, G. (1982) Endogenous phospholipid metabolism in stimulated neutrophils differential activation by FMLP and PMA, *Biochem Biophys Res Commun.* **107**, 951-8.
18. Tamura, M., Tamura, T., Tyagi, S. R. & Lambeth, J. D. (1988) The superoxide-generating respiratory burst oxidase of human neutrophil plasma membrane. Phosphatidylserine as an effector of the activated enzyme, *J Biol Chem.* **263**, 17621-6.
19. Heyworth, P. G., Bohl, B. P., Bokoch, G. M. & Curnutte, J. T. (1994) Rac translocates independently of the neutrophil NADPH oxidase components p47phox and p67phox. Evidence for its interaction with flavocytochrome b558, *J Biol Chem.* **269**, 30749-52.
20. Heyworth, P. G., Curnutte, J. T., Nauseef, W. M., Volpp, B. D., Pearson, D. W., Rosen, H. & Clark, R. A. (1991) Neutrophil nicotinamide adenine dinucleotide phosphate oxidase assembly. Translocation of p47-phox and p67-phox requires interaction between p47-phox and cytochrome b558, *J Clin Invest.* **87**, 352-6.
21. Quinn, M. T., Evans, T., Loetterle, L. R., Jesaitis, A. J. & Bokoch, G. M. (1993) Translocation of Rac correlates with NADPH oxidase activation. Evidence for equimolar translocation of oxidase components, *J Biol Chem.* **268**, 20983-7.
22. Pick, E. (2020) Cell-Free NADPH Oxidase Activation Assays: A Triumph of Reductionism, *Methods Mol Biol.* **2087**, 325-411.
23. Seifert, R. & Schultz, G. (1987) Fatty-acid-induced activation of NADPH oxidase in plasma membranes of human neutrophils depends on neutrophil cytosol and is potentiated by stable guanine nucleotides, *Eur J Biochem.* **162**, 563-9.
24. Swain, S. D., Helgerson, S. L., Davis, A. R., Nelson, L. K. & Quinn, M. T. (1997) Analysis of activation-induced conformational changes in p47phox using tryptophan fluorescence spectroscopy, *The Journal of biological chemistry.* **272**, 29502-10.
25. Shiose, A. & Sumimoto, H. (2000) Arachidonic acid and phosphorylation synergistically induce a conformational change of p47phox to activate the phagocyte NADPH oxidase, *The Journal of biological chemistry.* **275**, 13793-801.
26. Uhlinger, D. J., Taylor, K. L. & Lambeth, J. D. (1994) p67-phox enhances the binding of p47-phox to the human neutrophil respiratory burst oxidase complex, *J Biol Chem.* **269**, 22095-8.
27. Karimi, G., Houee Levin, C., Dagher, M. C., Baciou, L. & Bizouarn, T. (2014) Assembly of phagocyte NADPH oxidase: A concerted binding process?, *Biochimica et biophysica acta.* **1840**, 3277-83.
28. Suh, C.-I., Stull, N. D., Li, X. J., Tian, W., Price, M. O., Grinstein, S., Yaffe, M. B., Atkinson, S. & Dinauer, M. C. (2006) The phosphoinositide-binding protein p40phox activates the NADPH oxidase during FcgammaIIA receptor-induced phagocytosis, *The Journal of experimental medicine.* **203**, 1915-25.
29. Karathanassis, D., Stahelin, R. V., Bravo, J., Perisic, O., Pacold, C. M., Cho, W. & Williams, R. L. (2002) Binding of the PX domain of p47(phox) to phosphatidylinositol 3,4-bisphosphate and phosphatidic acid is masked by an intramolecular interaction, *EMBO J.* **21**, 5057-68.
30. Ueyama, T., Eto, M., Kami, K., Tatsuno, T., Kobayashi, T., Shirai, Y., Lennartz, M. R., Takeya, R., Sumimoto, H. & Saito, N. (2005) Isoform-specific membrane targeting mechanism of Rac during Fc gamma R-mediated phagocytosis: positive charge-dependent and independent targeting mechanism of Rac to the phagosome, *Journal of immunology (Baltimore, Md : 1950).* **175**, 2381-90.
31. Berdichevsky, Y., Mizrahi, A., Ugolev, Y., Molshanski-Mor, S. & Pick, E. (2007) Tripartite chimeras comprising functional domains derived from the cytosolic NADPH oxidase components p47phox, p67phox, and Rac1 elicit activator-independent superoxide production by phagocyte membranes: an essential role for anionic membrane phospholipids, *The Journal of biological chemistry.* **282**, 22122-39.
32. Stahelin, R. V., Burian, A., Bruzik, K. S., Murray, D. & Cho, W. (2003) Membrane binding mechanisms of the PX domains of NADPH oxidase p40phox and p47phox, *J Biol Chem.* **278**, 14469-79.
33. Li, X. J., Marchal, C. C., Stull, N. D., Stahelin, R. V. & Dinauer, M. C. (2010) p47phox Phox homology domain regulates plasma membrane but not phagosome neutrophil NADPH oxidase activation, *J Biol Chem.* **285**, 35169-79.
34. Yeung, T., Gilbert, G. E., Shi, J., Silvius, J., Kapus, A. & Grinstein, S. (2008) Membrane phosphatidylserine regulates surface charge and protein localization, *Science.* **319**, 210-3.
35. Sarfstein, R., Gorzalczany, Y., Mizrahi, A., Berdichevsky, Y., Molshanski-Mor, S., Weinbaum, C., Hirshberg, M., Dagher, M.-C. & Pick, E. (2004) Dual role of Rac in the assembly of NADPH oxidase, tethering to the membrane and activation of p67phox: a study based on mutagenesis of p67phox-Rac1 chimeras, *The Journal of biological chemistry.* **279**, 16007-16.
36. Faure, M. C., Sulpice, J. C., Delattre, M., Lavielle, M., Prigent, M., Cuif, M. H., Melchior, C., Tschirhart, E., Nusse, O. & Dupre-Crochet, S. (2013) The recruitment of p47(phox) and Rac2G12V at the phagosome is transient and phosphatidylserine dependent, *Biol Cell.* **105**, 501-18.
37. Magalhaes, M. A. & Glogauer, M. (2010) Pivotal Advance: Phospholipids determine net membrane surface charge resulting in differential localization of active Rac1 and Rac2, *J Leukoc Biol.* **87**, 545-55.
38. Valenta, H., Dupre-Crochet, S., Abdesselem, M., Bizouarn, T., Baciou, L., Nusse, O., Deniset-Besseau, A. & Erard, M. (2022) Consequences of the constitutive NOX2 activity in living cells: Cytosol acidification, apoptosis, and localized lipid peroxidation, *Biochim Biophys Acta Mol Cell Res.* **1869**, 119276.
39. Mizrahi, A., Berdichevsky, Y., Casey, P. J. & Pick, E. (2010) A prenylated p47phox-p67phox-Rac1 chimera is a Quintessential NADPH oxidase activator: membrane association and functional capacity, *The Journal of biological chemistry.* **285**, 25485-99.
40. Masoud, R., Bizouarn, T. & Houee-Levin, C. (2014) Cholesterol: A modulator of the phagocyte NADPH oxidase activity - A cell-free study, *Redox Biol.* **3**, 16-24.
41. Bizouarn, T., Souabni, H., Serfaty, X., Bouraoui, A., Masoud, R., Karimi, G., Houee-Levin, C. & Baciou, L. (2019) A Close-Up View of the Impact of Arachidonic Acid on the Phagocyte NADPH Oxidase, *Methods Mol Biol.* **1982**, 75-101.
42. Serfaty, X., Lefrancois, P., Houee-Levin, C., Arbault, S., Baciou, L. & Bizouarn, T. (2021) Impacts of vesicular environment on Nox2 activity measurements in vitro, *Biochim Biophys Acta Gen Subj.* **1865**, 129767.
43. Jesorka, A., Stepanyants, N., Zhang, H., Ortmen, B., Hakonen, B. & Orwar, O. (2011) Generation of phospholipid vesicle-nanotube networks and transport of molecules therein, *Nat Protoc.* **6**, 791-805.
44. Zhen, L., King, A. A., Xiao, Y., Chanock, S. J., Orkin, S. H. & Dinauer, M. C. (1993) Gene targeting of X chromosome-linked chronic granulomatous disease locus in a human myeloid leukemia

cell line and rescue by expression of recombinant gp91phox, *Proc Natl Acad Sci U S A.* **90**, 9832-6.
45. Chiba, T., Kaneda, M., Fujii, H., Clark, R. A., Nauseef, W. M. & Kakinuma, K. (1990) Two cytosolic components of the neutrophil NADPH oxidase, P47-phox and P67-phox, are not flavoproteins, *Biochem Biophys Res Commun.* **173**, 376-81.
46. Ebisu, K., Nagasawa, T., Watanabe, K., Kakinuma, K., Miyano, K. & Tamura, M. (2001) Fused p47phox and p67phox truncations efficiently reconstitute NADPH oxidase with higher activity and stability than the individual components, *The Journal of biological chemistry.* **276**, 24498-505.
47. Kreck, M. L., Freeman, J. L., Abo, A. & Lambeth, J. D. (1996) Membrane association of Rac is required for high activity of the respiratory burst oxidase, *Biochemistry.* **35**, 15683-92.
48. Masoud, R., Serfaty, X., Erard, M., Machillot, P., Karimi, G., Hudik, E., Wien, F., Baciou, L., Houee-Levin, C. & Bizouarn, T. (2017) Conversion of NOX2 into a constitutive enzyme in vitro and in living cells, after its binding with a chimera of the regulatory subunits, *Free Radic Biol Med.* **113**, 470-477.
49. el Benna, J., Ruedi, J. M. & Babior, B. M. (1994) Cytosolic guanine nucleotide-binding protein Rac2 operates in vivo as a component of the neutrophil respiratory burst oxidase. Transfer of Rac2 and the cytosolic oxidase components p47phox and p67phox to the submembranous actin cytoskeleton during oxidase activation, *J Biol Chem.* **269**, 6729-34.
50. Bizouarn, T., Karimi, G., Masoud, R., Souabni, H., Machillot, P., Serfaty, X., Wien, F., Refregiers, M., Houee-Levin, C. & Baciou, L. (2016) Exploring the arachidonic acid-induced structural changes in phagocyte NADPH oxidase p47(phox) and p67(phox) via thiol accessibility and SRCD spectroscopy, *FEBS J.* **283**, 2896-910.
51. Ugolev, Y., Molshanski-Mor, S., Weinbaum, C. & Pick, E. (2006) Liposomes comprising anionic but not neutral phospholipids cause dissociation of Rac(1 or 2) x RhoGDI complexes and support amphiphile-independent NADPH oxidase activation by such complexes, *J Biol Chem.* **281**, 19204-19.
52. Glogauer, M., Marchal, C. C., Zhu, F., Worku, A., Clausen, B. E., Foerster, I., Marks, P., Downey, G. P., Dinauer, M. & Kwiatkowski, D. J. (2003) Rac1 deletion in mouse neutrophils has selective effects on neutrophil functions, *J Immunol.* **170**, 5652-7.
53. Kim, C. & Dinauer, M. C. (2006) Impaired NADPH oxidase activity in Rac2-deficient murine neutrophils does not result from defective translocation of p47phox and p67phox and can be rescued by exogenous arachidonic acid, *Journal of leukocyte biology.* **79**, 223-34.
54. Kim, C. & Dinauer, M. C. (2001) Rac2 is an essential regulator of neutrophil nicotinamide adenine dinucleotide phosphate oxidase activation in response to specific signaling pathways, *J Immunol.* **166**, 1223-32.
55. Hata, K., Ito, T., Takeshige, K. & Sumimoto, H. (1998) Anionic amphiphile-independent activation of the phagocyte NADPH oxidase in a cell-free system by p47phox and p67phox, both in C terminally truncated forms. Implication for regulatory Src homology 3 domain-mediated interactions, *The Journal of biological chemistry.* **273**, 4232-6.
56. Nisimoto, Y., Ogawa, H., Miyano, K. & Tamura, M. (2004) Activation of the flavoprotein domain of gp91phox upon interaction with N-terminal p67phox (1-210) and the Rac complex, *Biochemistry.* **43**, 9567-75.
57. Miyano, K., Fukuda, H., Ebisu, K. & Tamura, M. (2003) Remarkable stabilization of neutrophil NADPH oxidase using RacQ61L and a p67phox-p47phox fusion protein, *Biochemistry.* **42**, 184-90.
58. van Bruggen, R., Anthony, E., Fernandez-Borja, M. & Roos, D. (2004) Continuous translocation of Rac2 and the NADPH oxidase component p67(phox) during phagocytosis, *J Biol Chem.* **279**, 9097-102.

Supplementary materials

Figure S1

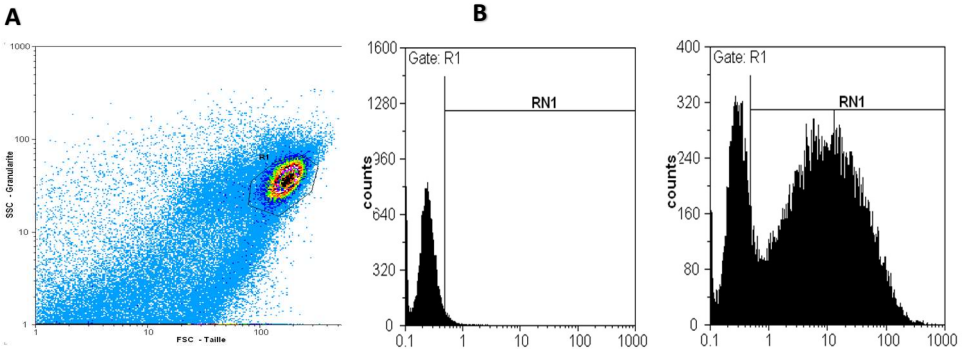

Figure S1. Fluorescence of untransfected cells and transfected cells. *To distinguish between the fluorescence due to trimeras from the intrinsic cellular fluorescence, untransfected cells are examined as negative control.* ***(A)*** *Cell identification based forward scatter (FSC) and size scatter (SSC) parameters.* ***(B)*** *Fluorescence histograms of untransfected cells (left) and transfected cells (right). In the left, the untransfected cells present an autofluorescence peak. The PLB985 cells that expressed the pEcitrine- trimer present a fluorescence above the autofluorescence in the RN1 window.*

Figure S2

MGDTFIRHIALLGFEKRFVPSQHYVYMFLVKWQDLSEKVVYRRFTEIYEFHKTLKEMFPIEAGAINPENRIIPHLPAPKWFDGQR
AAENRQGTLTEYCSTLMSLPTKISRCPHLLDFFKVRPDDLKLPTDNQTKKPETYLMPKDGKSTATDITGPIILQTYRAIADYEKTS
GSEMALSTGDVVEVVEKSESGWWFCQMKAKRGWIPASFLEPLDSPDETEDPEPNYAGEPYVAIKAYTAVEGDEVSLLEGEAVE
VIHKLLDGWWVIRKDDVTGYFPSMYLQKSGQDAAASTGGGSSMSLVEAISLWNEGVLAADKKDWKGALDAFSAVQDPHSRIC
FNIGCMYTILKNMTEAEKAFTRSINRDKHLAVAYFQRGMLYYQTEKYDLAIKDLKEALIQLRGNQLIDYKILGLQFKLFACEVLYN
IAFMYAKKEEWKKAEEQLALATSMKSEPRHSKIDKAMECVWKQKLYEPVVIPVGKLFRPNERQVAQLAKKDYLGKATVVASVV
DQDMQAIKCVVVGDGAVGKTCLLISYTTNAFPGEYIPTVFDNYSANVMVDGKPVNLGLWDTAGLEDYDRLRPLSYPQTDVFLI
CFSLVSPASFENVRAKWYPEVRHHCPNTPIILVGTKLDLRDDKDTIEKLKEKKLTPITYPQGLAMAKEIGAVKYLECSALTQRGLK
TVFDEAIRAVLCPPPVKKRKRKRLLL

Figure S2: Amino acid sequence of the prototype-trimera*. The sequence of p47N (1-286) is in red, the one of p67N (1-212) is in green and the one of Rac1Q61L (1-192) is in blue. The PX domain is highlighted in grey with the residues involved in PPL binding in yellow, the SH3 domains in green, the polybasic region of Rac1 in blue and the prenylated cysteine residue in pink.*

Figure S3

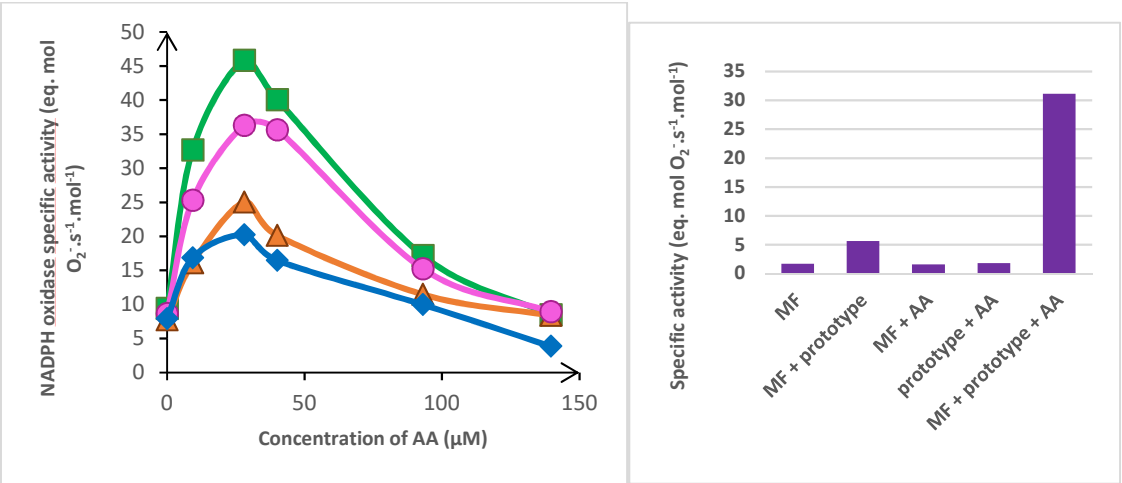

Figure S3*: **AA-dependence of NADPH oxidase activation by GFP-trimeras using PLB-985 membranes, in cell-free assays.*** ***(A)*** *NADPH oxidase activity as function of AA concentration. PLB-985 MF was mixed with 300 nM of the following GFP-trimera: prototype trimera (■); GFP-trimera p47^{phox} ΔPX (▲); GFP-trimera Rac1-PB2 (●); GFP-trimera Rac1-PB6Q (♦) and an increasing concentration of AA. Superoxide anion production was initiated by the addition of NADPH (200 µM). (B) Set of controls, when indicated the activity was measured in presence of MF (4 nM cyt b$_{558}$), prototype trimera (300 nM) and AA (40µM). Measurements were performed as described in the material and methods section. Each point is the mean of the results obtained from three different membrane fractions. The standard error corresponds to around 10% of the rate values.*